Percolation model of immiscible displacement in the presence of buoyancy forces

David Wilkinson
Schlumberger-Doll Research, P.O. Box 307, Ridgefield, Connecticut 06877
(Received 20 October 1983)

We consider the quasistatic displacement of a nonwetting fluid by a wetting one in a porous medium in the presence of buoyancy forces. A simple percolation model of this process is presented and analyzed both theoretically and by Monte Carlo simulation. It is shown that the fact that percolation is a critical phenomenon, with diverging correlation length at the critical point, has a significant effect on the physics of the system, in particular on the dependence of nonwetting phase residual saturation on the density contrast between the phases. An extension of these ideas to the case where the pressure field is generated by viscous rather than buoyancy forces is suggested.

I. INTRODUCTION

In this paper we consider the process of immiscible displacement of a nonwetting fluid by a wetting one from a porous medium. For convenience we will refer to the wetting fluid as water and the nonwetting fluid as oil, although in principle our discussion is applicable to any two fluids with the appropriate wetting characteristics.[1] The medium is considered to be initially 100% saturated with oil, except possibly for small traces of "connate" water, and is then subjected to a laboratory waterflood. We shall consider for simplicity the case where the sample is long compared to its width, so that the flood is essentially one dimensional, though this is not a crucial feature of the discussion. As the water advances into the medium, it is possible for it to completely surround regions of oil, which subsequently remain trapped as "residual oil." Two entirely different entrapment mechanisms have been identified in the literature.[2]

(1) Trapping in single pores due to snap-off processes. Here the net result is that water entering a given pore does not completely displace the oil, but rather occupies only the walls of the pore, leaving some isolated oil in the center. This is an essentially local phenomenon, depending on the detailed geometry of the pore and possibly on the nature and extent of connate water films.

(2) Bypassing of one or more pores by the water phase. In this case an entire cluster of pores remains completely full of oil. This process is a larger-scale phenomenon controlled by the random multiply connected topology of the pore space.

The present paper is concerned entirely with the second scenario, and in particular with the nature of the larger trapped clusters; in a material where both mechanisms operate, this analysis will refer only to that part of the residual saturation which is caused by bypassing. In recent years many authors[3–9] have invoked the mathematical theory of percolation to describe the statistical nature of this bypassing process. This theory is strictly applicable only in the limit of infinitesimal flow rate where viscous forces may be completely neglected, and the system is dominated by capillary (surface tension) forces. In this situation percolation ideas predict[8,9] that the clusters of residual oil exist on all size scales; more specifically, if we define $n(s)$ to be the number of clusters containing s pores, then for large s

$$n(s) \sim s^{-\tau} , \tag{1.1}$$

where $\tau \sim 2.07$ is a critical exponent which we expect to be universal for all dimensional systems. If we normalize $n(s)$ to the total number of pores in the sample and estimate the residual oil saturation S_{or} by counting the fraction of pores containing oil (i.e., we ignore the size variation of the pores), then

$$S_{or} = \sum_{s=1}^{\infty} s n(s) . \tag{1.2}$$

Since the value of τ is close to but slightly larger than 2, the sum (1.2) converges, but slowly, so that the residual oil saturation receives contributions from clusters over a wide size range.

It is not the purpose of this paper to present an extensive justification of the percolation approach, but rather to explore the consequences of these ideas in the realistic situation where the forces of viscosity or buoyancy are acting in addition to surface tension. In the viscous case there is a dimensionless parameter, the capillary number, which represents the competition between viscous and capillary forces. Let us estimate the viscous pressure drop across a typical grain size R using the water viscosity μ_w, the superficial (Darcy) velocity v, and the absolute permeability k:

$$\Delta p_{\text{visc}} \sim \frac{\mu_w v R}{k} . \tag{1.3}$$

Comparing this to a typical interfacial pressure difference

$$\Delta p_{\text{int}} \sim \frac{\gamma}{R} , \tag{1.4}$$

where γ is the interfacial tension, we obtain

$$\frac{\Delta p_{\text{visc}}}{\Delta p_{\text{int}}} \sim \frac{N_{\text{cap}}}{K} , \tag{1.5}$$

where

$$N_{\text{cap}} = \frac{\mu_w v}{\gamma} \tag{1.6}$$

is the capillary number expressed in terms of the superficial velocity v, and K is a dimensionless geometrical constant given by

$$K = \frac{k}{R^2} . \tag{1.7}$$

Since the permeability k is dominated by the narrow constrictions (throats) in the medium, the constant K is typically rather small, of order 10^{-3}. When N_{cap} is finite there is a characteristic length, the capillary length L_{cap}, which represents the distance over which viscous pressure differences become comparable to interfacial pressure differences. If we measure this length in units of a typical grain size R, then

$$\frac{L_{\text{cap}}}{R} \sim \frac{K}{N_{\text{cap}}} . \tag{1.8}$$

It is known experimentally that as the capillary number increases, the residual oil saturation decreases. Typical experimental curves are shown in Fig. 1.[10] The two curves, labeled a and b represent entirely different experimental procedures. The connected curve, labeled b, is the result obtained by performing the displacement experiment at a given capillary number with the sample initially 100% saturated with oil, i.e., the oil is initially in a single connected cluster. Each point on curve b represents a separate experiment. The disconnected curve, labeled a, is obtained by steadily increasing the capillary number in a single experiment, starting with the oil in disconnected clusters, i.e., in the configuration obtained at the end of a type-b experiment. We see that curve b is unique, but that there are many curves a, one for each value of the capillary number of the initial flood. Typically, as in Fig. 1, only one curve a is reported, that corresponding to the lowest capillary number used in the study, but in principle there is a curve a corresponding to each of the data points on curve b.

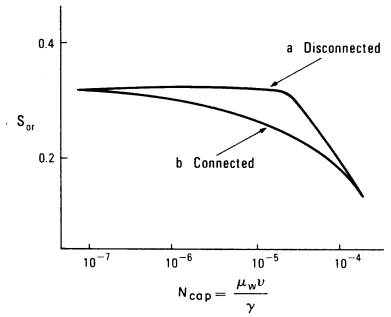

FIG. 1. Typical experimental curves for the dependence of residual oil saturation S_{or} on capillary number N_{cap}. The two curves represent different experimental procedures as explained in the text. Curves do not represent any particular experiment, but are typical of results quoted, for example, in Ref. 10.

In our percolation picture we may understand the qualitative features of these curves as follows. For curve a, one starts at low capillary number with disconnected oil clusters on a wide range of size scales. As the capillary number is increased, the larger blobs are unable to withstand the viscous pressure gradient and begin to move. However, it is widely believed that they are not expelled from the sample, but rather become broken up into smaller pieces which are stable at the existing flow rate.[11] Thus initially the residual oil saturation remains unchanged (the flat portion of the curve). As the flow rate is gradually increased, this process continues until all the clusters have been broken down into pieces which occupy a single pore. Further increase of the capillary number then results in displacement of oil from single pores, and the residual saturation decreases (the falling portion of the curve). The characteristic knee in the curve corresponds to the capillary number for which the capillary length (1.8) is comparable to a pore or grain size, i.e., $N_{\text{cap}} \sim K$.[12] We see that in this picture the shape of curve a has nothing to do with percolation concepts, but rather is due to local processes controlled by the geometry and size distribution of individual pores.

In the disconnected case, curve b, there is interesting structure at much lower capillary numbers, well below the value required for mobilization of blobs in a single pore. The shape of curve b is controlled by modification of the original entrapment mechanism, and it is reasonable to suppose that, at least at low flow rates, the main effect of a nonzero capillary number is on what would have been the larger trapped clusters had the flow rate been infinitesimal.

The idea of changing the residual saturation by cutting off the cluster size distribution in some way has been suggested in the important paper of Larson, Davis, and Scriven.[13] However, these authors apply this idea to the disconnected oil data, curve a, rather than the connected oil, curve b, as proposed here. In our language, their procedure consists of cutting off the size distribution (1.1) at some maximum size $s_{\max}$, where $s_{\max}$ is the typical size of clusters of length L_{cap}. This is in accord with the picture that once a cluster becomes unstable against mobilization it is expelled from the sample. As observed above, we do not believe this is what actually happens. However, even given this assumption, it should not be possible to fit a curve of type a in this way, because the power-law distribution (1.1) has no natural scale to provide the knee in the curve. It seems that the only reason Larson, Davis, and Scriven were able to "successfully" fit disconnected oil data is that they used a cluster size distribution taken from percolation simulations on a $30\times30\times30$ lattice. The knee in their fitted curve corresponds to a capillary number for which the capillary length is approximately 30 pore lengths.

In the remainder of this paper we will discuss only the case of displacement of connected oil, i.e., the type-b experiment where the sample is initially fully saturated with oil. In order to investigate this question in detail we will first consider the related problem of quasistatic imbibition in the presence of buoyancy forces. This problem is similar to the viscous case in that it involves pressure fields

which vary as a function of position, but simpler in that these pressure fields are determined by purely hydrostatic rather than dynamic effects. If the density difference

$$\Delta\rho=\rho_w-\rho_0 \tag{1.9}$$

is positive, and the water is introduced from below as in Fig. 2, then the process of imbibition is hindered by the buoyancy effects. In this situation there is a dimensionless number, the Bond number, which represents the competition between buoyancy and capillary forces. Over a typical grain size R, the hydrostatic pressure difference between the phase changes by an amount

$$\Delta p_{\text{grav}}\sim\Delta\rho g R\ . \tag{1.10}$$

Comparing this to a typical interfacial pressure difference (1.4) we obtain

$$\frac{\Delta p_{\text{grav}}}{\Delta p_{\text{int}}}\sim\frac{\Delta\rho g R^2}{\gamma}\equiv B\ . \tag{1.11}$$

The ratio (1.11) is conventionally called the Bond number. Just as in the viscous case there is a capillary length, which here represents the distance over which buoyancy pressure differences are comparable to interfacial pressure differences. Measured in units of the grain size we have

$$\frac{L_{\text{cap}}}{R}\sim\frac{1}{B}\ . \tag{1.12}$$

We see that the Bond number is roughly equivalent to the ratio N_{cap}/K in (1.5). A more precise correspondence for the purpose of determining the residual oil saturation will be suggested in Sec. III.

The main results of this paper take the form of universal scaling formulas for the maximum cluster length $L_{\max}$ and residual oil saturation S_{or} which are valid in the limit of small Bond number B. Specifically we find

$$\frac{L_{\max}}{R}\sim\left[\frac{1}{B}\right]^{\mu}, \tag{1.13}$$

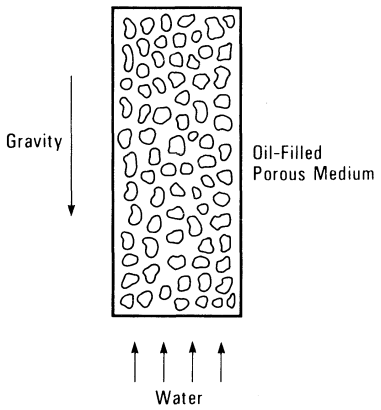

FIG. 2. Schematic drawing of a quasistatic imbibition experiment in the presence of buoyancy. The heavier fluid, water, is introduced from below at very low flow rate, and the oil escapes via the upper face of the sample. Sides of the sample are impermeable.

and

$$S^*_{\text{or}}-S_{\text{or}}\sim B^{\lambda}\ , \tag{1.14}$$

where S^*_{or} is the value at $B=0$, and the exponents take the approximate values $\mu\sim0.47$ and $\lambda\sim0.77$.

In Sec. II we present and analyze a simple quasistatic model for imbibition in the presence of buoyancy. The results (1.13) and (1.14), and the values of the exponents λ and μ, are obtained theoretically in terms of percolation exponents, and confirmed directly by Monte Carlo computer simulations of the model. In Sec. III we indicate briefly how these ideas might be extended to the case where the pressure field is generated by viscous effects rather than buoyancy. Section IV contains a discussion of the results.

II. BUOYANCY MODEL

The application of percolation ideas to immiscible displacement rests on two crucial assumptions.

(1) The motion of the oil-water interface consists of a discrete sequence of jumps of individual menisci at locations which are determined purely by surface tension effects.

(2) The pore space is multiply connected and in some sense random.

The actual model we will consider is probably the simplest possible one which realizes these ideas, and as such is necessarily somewhat naive. Nevertheless, we believe it captures some essential features of the problem, which might be obscured in a more realistic and complicated model. One reason a naive model can give useful information is that percolation is a critical phenomenon with universal behavior in the critical region; for example, the size distribution (1.1) has an exponent τ which should be independent of local details of the geometry such as coordination number and pore size distribution.

We consider a geometric model for the medium which consists of pores joined together by narrower connecting throats. In an imbibition process (water displacing oil), interfacial pressures always drive the oil-water interfaces through the throats, but at a given pressure difference between the phases (capillary pressure)

$$p_{\text{cap}}=p_0-p_w \tag{2.1}$$

the water can penetrate only the smaller pores. For given p_{cap} let q represent the "allowed water fraction," i.e., the fraction of pores which could become water filled, given that one or more of their neighboring pores contained water. (Note that this is not the same as the water saturation S_w, since not all allowed pores are accessible.) Let us express the relationship between p_{cap} and q as

$$p_{\text{cap}}=\frac{\gamma}{R}f(q)\ , \tag{2.2}$$

where R is a typical grain size and $f(q)$ is dimensionless and of order unity. The function $f(q)$ is positive and monotonically decreasing, and contains information about the pore size distribution of the material. If we assume that the pores are statistically independent, we may implement this idea in a model by assigning a random number

r, drawn from a uniform distribution on the unit interval $0 \leq r < 1$, to each pore. A pore assigned random number r can be filled when the capillary pressure p_{cap} falls below a threshold value p_{thresh} given by

$$p_{\text{thresh}} = \frac{\gamma}{R} f(r) . \tag{2.3}$$

At a given capillary pressure p_{cap}, i.e., a given allowed fraction q, those pores with $p_{\text{thresh}} > p_{\text{cap}}$, i.e., those with $r < q$, are allowed.

In the absence of buoyancy, the quasistatic model we discuss is based on the physical picture that at any given instant the system is in hydrostatic equilibrium; the pressure in each phase, and hence the capillary pressure, is everywhere constant. The oil-water menisci in the system all have the same curvature and are assumed to be in stable configurations. As the water advances due to the externally applied infinitesimal flow rate, the capillary pressure gradually decreases and the menisci adjust themselves adiabatically, until such time as the capillary pressure reaches the threshold pressure for one of the pores to fill. At this point the meniscus in the pore in question finds itself in an unstable configuration, and moves rapidly at a rate which is determined not by the bulk flow but rather by the local competition between capillary, viscous, and inertial forces. Such rapid motions are known as Haines jumps.[14] The present model does not attempt to treat these motions, but simply assumes that the net effect is that the pore in question fills with water, the pressure in the water phase drops, and the system again comes to hydrostatic equilibrium. These processes are assumed to occur instantaneously compared to the time scale of the bulk flow. Based on these ideas we may construct a simple percolation model of the displacement process as follows.

(1) The medium is represented as a regular lattice structure in which the sites represent pores and the bonds represent throats. The lattice spacing represents the grain size R. Each pore is assigned a random number r, drawn from a uniform distribution on the unit interval [0,1], which specifies the pressure at which it can fill with water, according to (2.3).

(2) The lattice is initially filled with oil, and water is introduced from one face. The sides of the lattice are treated as impermeable barriers, or alternatively periodic boundary conditions are imposed. The displaced oil escapes from the opposite face of the lattice.

(3) The advance of the water into the oil consists of a sequence of discrete steps in which at each stage the water displaces the oil from that pore on the interface which has the highest threshold capillary pressure, i.e., the one with the smallest assigned random number.

(4) Regions of oil which are surrounded by water cannot be invaded, and remain trapped as residual oil.

(5) The process stops when all remaining oil is contained in these trapped clusters.

The rules above describe a variant of percolation theory which has become known as invasion percolation.[8,9,15] Although there is no reference to the allowed water fraction in the algorithm for invasion percolation, one finds, for a large system, that at any stage in the process the water has occupied only sites with random numbers r below some threshold value q, and it is natural to identify this q as the allowed water fraction. This leads to many similarities between invasion percolation and ordinary percolation. However, there are also some important differences.

(1) The invading water in invasion percolation consists of a single connected cluster in accordance with the nature of the displacement process. By contrast, in ordinary percolation one normally fill all sites in the lattice with probability q (i.e., one fills all those with random number $r \leq q$), thus producing many disjoint water clusters. This can be circumvented by simply declaring that only those clusters which are accessible to the inlet face are actually filled with water. However, one then has the problem that there is no specified order in which the sites are filled, and it is impossible to decide unambiguously which regions of the oil phase become trapped. This difficulty does not arise in invasion percolation, which describes a unique time sequence of advances of the interface, and hence a unique way of determining the trapping configurations.

(2) Because the rules of invasion percolation specify that regions of oil which are surrounded are not subsequently invaded, one finds at any stage that not all the accessible sites with $r \leq q$ have been invaded because some of them were already trapped at the time when they would otherwise have been chosen. One consequence of this is that regions of oil which become trapped at high capillary pressures, i.e., low values of q, do not become smaller as q is increased. Thus the final distribution of trapped oil clusters consists of clusters produced at many different q values, and cannot be simply described in terms of ordinary percolation.

The main results in invasion percolation in three dimensions relevant to our purpose are the following.[8,9]

(1) As the simulation proceeds, the allowed water fraction q steadily increases. Except in the very early stages, there is no flood front as in a viscosity dominated flood, but rather the water first fills the entire sample at a low saturation, and then grows in a statistically homogeneous and isotropic fashion.

(2) At breakthrough, i.e., when the water first forms a connected path across the sample, the water is at percolation threshold, and the allowed water fraction q takes the value q_c, the percolation threshold for the lattice. Up to this point there is very little trapping, and the only trapped clusters are very small. The water occupies a single percolation cluster at threshold and so is a fractal set; if the simulation is performed on a sample of linear dimension L, then the water saturation (the fraction of sites occupied by water) shows a finite size scaling behavior

$$S_w \sim \left[\frac{L}{R} \right]^{-\alpha} , \tag{2.4}$$

where the exponent α is related to the fractal dimension D and space dimension d by

$$\alpha = d - D . \tag{2.5}$$

For $d=3$ we find $\alpha \sim 0.5$, i.e., $D \sim 2.5$, in agreement with the accepted fractal dimension 2.49 in ordinary percolation.[16]

(3) As the water saturation increases, more trapping takes place and larger trapped clusters are created. Eventually all the remaining oil is in trapped clusters and the process ends. At this point the oil is at percolation threshold, and the allowed water fraction q equals $1-q_c$. For a medium represented by a simple cubic lattice, the residual oil saturation S_{or}^* (the fraction of sites containing oil) found in computer simulations is approximately

$$S_{or}^* = 0.341 , \tag{2.6}$$

which is comparable to but somewhat larger than the percolation threshold 0.312 for a simple cubic lattice. The cluster size distribution shows the power-law behavior (1.1) discussed in the Introduction. This behavior is expected to be universal, and illustrates the absence of any finite length scale at the percolation threshold. [Of course in practice the distribution (1.1) is cut off by the finite sample size.] The exponent $\tau \sim 2.07$ found in the Monte Carlo simulations is somewhat smaller than the value 2.20 observed in ordinary percolation;[16] this may be due to the fact that the clusters in invasion percolation are formed over a range of q values as discussed above.

Note that in order for the above description to make sense, it is necessary that q_c be less than $1-q_c$, i.e., $q_c < \frac{1}{2}$. This is always the case for a three-dimensional system, but for a planar two-dimensional system one always has $q_c \geq \frac{1}{2}$ because the two species cannot percolate together. If one wishes for convenience to use a two-dimensional representation of the medium, it is necessary to use a nonplanar structure in order to observe the correct qualitative behavior. Examples of such structures are the lattice obtained by inserting all the diagonals on a square lattice (coordination number 8), or that obtained by stacking two square lattices (coordination number 5).

In the presence of buoyancy we may generalize the above model by assuming that at any instant the system is in vertical equilibrium, so that the capillary pressure depends linearly on height x:

$$p_{cap}(x) - p_{cap}(x=0) = \Delta\rho g x . \tag{2.7}$$

Given such a capillary pressure field we define a jump potential[2] for each pore on the interface by

$$p_{jump} = p_{thresh} - p_{cap}(x)$$
$$= \frac{\gamma}{R} f(r) - \Delta\rho g x + \text{const} , \tag{2.8}$$

where r is the random number assigned to the pore, x is its vertical height, and $f(r)$ is the function introduced in (2.2). The pore which fills is now the one with the largest jump potential rather than simply that with the largest threshold pressure.

In the presence of this vertical bias, the system at any time is no longer statistically homogeneous, but rather there is a well-defined transition region as shown schematically in Fig. 3. At the top of the transition zone, the water is at percolation threshold and the allowed water fraction q is q_c. At the bottom of this zone, the oil is at percolation threshold and q equals $1-q_c$. Below the transition region, the oil is completely disconnected. By considering the values of the capillary pressure at the top and bottom of the zone, it is easy to see that the height h of the transition zone is given by

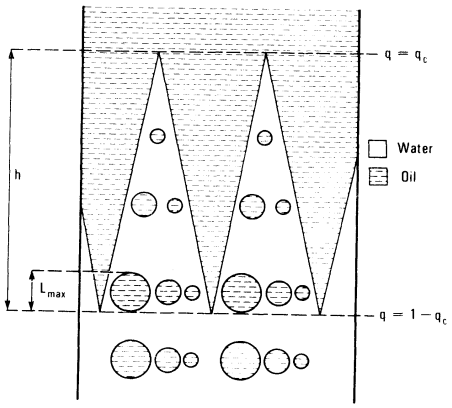

FIG. 3. Schematic picture of the transition zone in a buoyancy-hindered flood. Figure does not mean to indicate the shapes of the clusters, which are fractal-like objects, but merely the connectedness properties and relative cluster size as a function of height. Each vertical position represents a stage of evolution of the system, the top of the transition zone being at an early stage and the bottom at a later stage. Cluster size distribution at any height consists of the clusters "inherited" from earlier stages of evolution, together with new clusters being generated at that height, the latter being typically larger than the former. At any time, as shown in figure, the largest clusters, of length L_{max}, are those being created at the bottom of the zone.

$$\frac{h}{R} = \frac{f(q_c) - f(1-q_c)}{B} , \tag{2.9}$$

where B is the Bond number (1.11). Since the function $f(q)$ is of order unity, we see

$$\frac{h}{R} \sim \frac{1}{B} \sim \frac{L_{cap}}{R} , \tag{2.10}$$

so that h is of order L_{cap} as one would expect.

We first consider how the buoyancy effects determine the maximum size of the trapped oil clusters. As indicated in Fig. 3, the largest clusters are created near the bottom of the zone where the oil is approaching percolation threshold. At some fixed time, let us consider an arbitrary location in the zone and define Δq by

$$q = 1 - q_c - \Delta q , \tag{2.11}$$

where q is the local value of the allowed water fraction at this position. Define L to be the local correlation length, i.e., the linear extent of the largest clusters being formed. In order for it to make sense to say that these clusters are being generated at a particular value of q, it must be that the change in q over a distance L is small compared to Δq, i.e.,

$$L \left| \frac{\partial q}{\partial x} \right| < \Delta q . \tag{2.12}$$

If this inequality is violated, it is meaningless to regard q as a macroscopic variable, since there is no region larger than the correlation length over which q remains effec-

tively constant. From (2.2) we have

$$\frac{\partial q}{\partial x}=\frac{R}{\gamma f'(q)}\frac{\partial p_{\rm cap}}{\partial x} \tag{2.13}$$

so that (2.12) reduces to

$$\frac{LR}{\gamma|f'(q)|}\frac{\partial p_{\rm cap}}{\partial x}<\Delta q\ . \tag{2.14}$$

Since $\partial p_{\rm cap}/\partial x$ equals $\Delta\rho g$ this may be expressed as

$$\frac{L}{R}\frac{B}{|f'(q)|}<\Delta q\ , \tag{2.15}$$

where B is the Bond number (1.11). Since $f'(q)$ is of order unity and we are considering small Bond numbers B, this inequality is always satisfied provided Δq is not too small, since outside the critical region the dimensionless correlation length L/R is of order unity. As $\Delta q\to 0$, however, the correlation length diverges, since oil clusters of arbitrarily large size are being created,

$$\frac{L}{R}\sim\Delta q^{-\nu}\ , \tag{2.16}$$

where ν is a critical exponent which we expect to be universal. We will assume that this exponent is the same as in ordinary percolation in three dimensions, i.e., $\nu\sim 0.88$.[16] Thus as $\Delta q\to 0$, i.e., as we approach the bottom of the transition zone, the inequality (2.15) is necessarily violated, no matter how small the Bond number B. If we convert (2.15) from an inequality to an equality, and use (2.16), we may estimate the value of Δq where (2.15) breaks down, and the corresponding maximum attainable correlation length $L_{\rm max}$

$$\frac{L_{\rm max}}{R}\sim\left[\frac{1}{B}\right]^{\mu} \tag{2.17}$$

with

$$\mu=\frac{\nu}{1+\nu}\sim 0.47\ , \tag{2.18}$$

where we have used the percolation value $\nu\sim 0.88$. Note that we have suppressed $f'(q)$, which should be evaluated at $q=1-q_c$, because it is of order unity. It is natural to assume that $L_{\rm max}$ is the maximum vertical extent of the trapped clusters formed; the fundamental result (2.17) indicates that this length scales as a fractional power of the inverse Bond number, as opposed to the capillary length $L_{\rm cap}$ (which measures the total height of the transition zone) which scales directly as the inverse Bond number.

The effect of this cutoff in the cluster size distribution on the residual oil saturation $S_{\rm or}$ is not so easy to determine. Unlike the scaling behavior of the maximum correlation length (2.17), this effect depends crucially on the distinction between invasion percolation and ordinary percolation. In the Appendix we present an argument, suggested to the author by Halperin, leading to the prediction that at finite Bond number B the residual oil saturation $S_{\rm or}$ differs from the value $S_{\rm or}^*$ obtained when $B=0$ by an amount which scales for small B as

$$S_{\rm or}^*-S_{\rm or}\sim B^{\lambda}\ , \tag{2.19}$$

where the exponent λ is related to the correlation length exponent ν and order parameter exponent β by

$$\lambda=\frac{1+\beta}{1+\nu}\sim 0.77\ , \tag{2.20}$$

where we have used the three-dimensional percolation values $\nu\sim 0.88$ and $\beta\sim 0.45$.[16] Although we do not give the details here, we observe that if one assumed that the power-law distribution (1.1) were simply cut off at a maximum size $s_{\rm max}$ corresponding to the maximum length $L_{\rm max}$ in (2.17), then the exponent λ in (2.19) would be much smaller, of order 0.25.

In order to check the above theoretical predictions we have performed Monte Carlo computer simulations of the model. Unlike the case with $B=0$ we see from (2.8) that it is necessary to know the function $f(q)$ in (2.2) in order to specify the time ordering of the jumps. In our simulations we have made the simple choice

$$f(q)=-q+\text{const} \tag{2.21}$$

which means that the threshold pressures of the pores are uniformly distributed. While this choice is clearly arbitrary, the universal predictions (2.17) and (2.19) should hold for any reasonable choice of $f(q)$.

In Fig. 4 we show the results of Monte Carlo simulations at three different Bond numbers. In each case both the breakthrough point and the final configuration are shown. The simulations were done on a nonplanar two-dimensional lattice obtained by inserting the diagonals on a square lattice; such a lattice has behavior qualitatively similar to the three-dimensional case but with two-dimensional critical exponents. We see that as the Bond

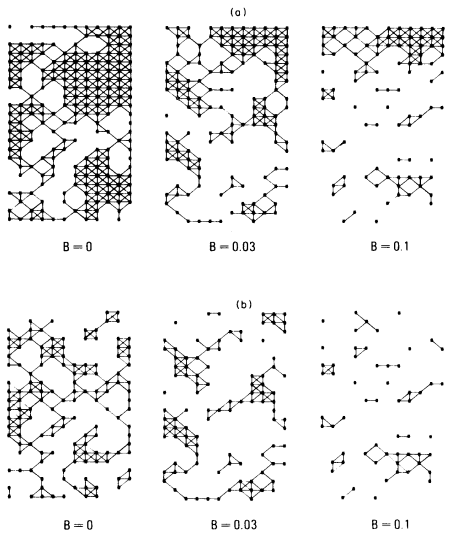

FIG. 4. Results of Monte Carlo simulations for three different Bond numbers. For each Bond number (a) is the breakthrough point and (b) is the final configuration when all the oil is trapped. Flow direction is from bottom to top. Samples in the three cases are taken from the same statistical distribution but are not identical. Connectedness of the lattice is that obtained by inserting all the diagonals on a square lattice. Sites marked with an asterisk contain oil, and the lines represent the connectedness of the oil phase.

number is increased, the transition zone becomes shorter and the largest clusters smaller. The total residual saturation decreases but the number of small clusters increases, so that the large clusters are not totally missing from the distribution, but rather get partially broken up into smaller ones. This observation, which we shall see confirmed in our three-dimensional numerical data, means that the decrease in residual saturation with increasing Bond number is not as rapid as one would otherwise expect.

Our actual numerical results are based on simulations on a $30\times30\times60$ simple cubic lattice with periodic boundary conditions on the sides. On such a finite lattice, there is a lower limit to the Bond number which can be studied, since at low enough B the largest clusters become limited by the lattice size rather than the buoyancy effects. For this reason we have considered only Bond numbers greater than 0.001. In order to investigate the maximum cluster size we have computed the moment ratios

$$L_k=\frac{\langle L^k\rangle}{\langle L^{k-1}\rangle}\ , \tag{2.22}$$

where $\langle L^k\rangle$ denotes the average of the kth power of the lengths of the clusters generated. Clearly, as $k\to\infty$ the L_k are dominated by the largest clusters. On the other hand, the statistics get worse because the moments are determined by fewer of the clusters in the sample, so that in practice, for a given range of B values, it is better to use a finite value for k. In Fig. 5 the quantity L_k for various k is plotted against the Bond number B. It is seen that the larger k values give reasonable straight lines on the log-log plot; for $k=4$, 6, 8, and 10 we obtain values 0.43, 0.50, 0.51, and 0.50 for the exponent μ in (2.18). This suggests that $k=6$ is already large enough for the range of B values considered here. We see that the value $\mu\sim0.50$ is in reasonable agreement with the theoretical prediction 0.47 based on percolation exponents.

The dependence of residual saturation on Bond number is shown in Fig. 6. As B increases, the residual oil saturation S_{or} decreases from its $B=0$ value $S^*_{or}=0.341$, falling to $S_{or}=0.241$ for $B=0.1$. Another way to plot the same data is shown in Fig. 7, where the difference $S^*_{or}-S_{or}$ is plotted as a function of B. The exponent $\lambda=0.76$ obtained from the plot is again in excellent agreement with the theoretical prediction $\lambda\sim0.77$.

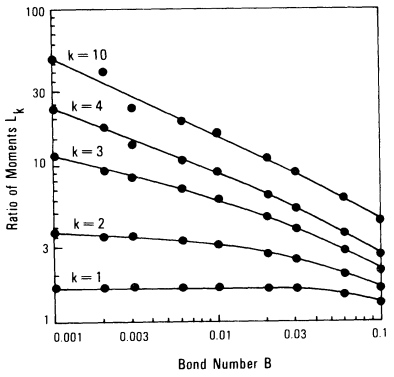

FIG. 5. Plot of the ratio of moments L_k [Eq. (2.22)] against Bond number B, for various values of k. Despite the progressively poorer statistics, it is seen that the larger k values yield a reasonable straight-line fit to the data.

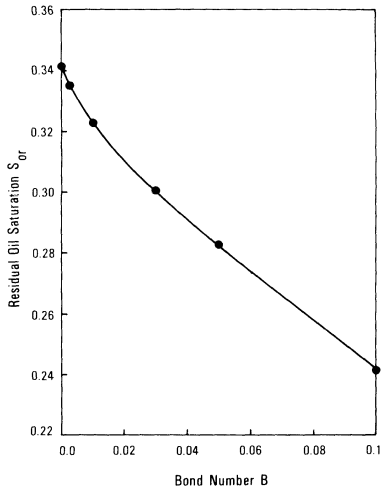

FIG. 6. Plot of the residual oil saturation S_{or} against Bond number B. In our simple model we estimate residual oil saturation by counting the fraction of pores containing oil at the end of the simulation. As B increases, S_{or} decreases from the value S^*_{or} obtained in the absence of buoyancy.

In Fig. 8 we have plotted the cluster size distribution for various values of B. We see that at nonzero B the distribution is cut off above a maximum size s_{max}, but that for $s<s_{max}$ the number of clusters exceeds that at $B=0$. The fact that the exponent λ is much larger than would be obtained by assuming that the distribution is simply cut off indicates that in fact these two effects exactly cancel to leading order in B.

III. VISCOUS CASE

In this section we suggest how the above analysis might be extended to the case where the pressure field is generated by viscous forces. This is a fundamentally more complicated problem than the buoyancy case, because the

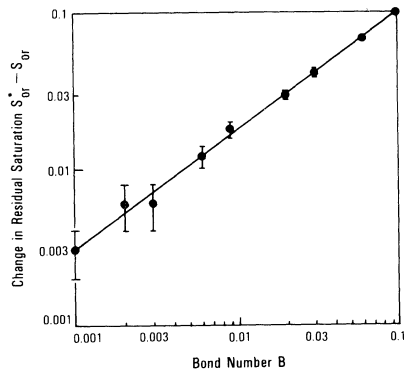

FIG. 7. Log-log plot of the change in residual saturation $S^*_{or}-S_{or}$ against Bond number B. Error bars represent one standard deviation.

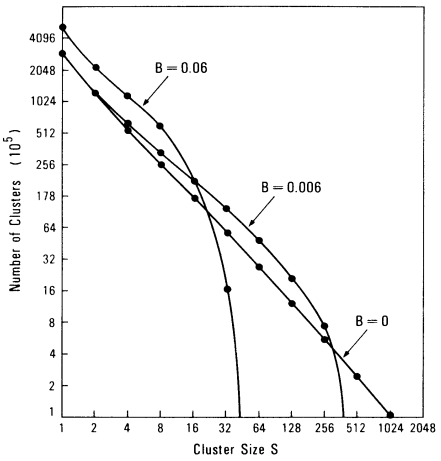

FIG. 8. Plot of the cluster size distribution $n(s)$. Plot is actually a logarithmic histogram, i.e., the value plotted for $\log_2 s = n$ is the number of clusters whose size s was in the range $2^n \leq s \leq 2^{n+1}-1$. Thus the slope of the straight portion of the $B=0$ curve is not $-\tau$ as in (1.1) but rather $1-\tau$. We see that for $B\neq 0$ the distribution is cut off above some $s_{\max}$ but for $s < s_{\max}$ the distribution exceeds that at $B=0$.

pressure variations in the system are dynamically determined by the fluid configurations rather than being purely hydrostatic. The picture we will adopt is a mean-field description in which each interface moves under the average pressure field produced by the motion of the others. In order to estimate the pressure fields we will use the one-dimensional version of the usual multiphase Darcy equations[17]

$$\frac{\partial p_w}{\partial x} = -\frac{\mu_w v_w}{k k_{rw}} , \tag{3.1}$$

$$\frac{\partial p_0}{\partial x} = -\frac{\mu_0 v_0}{k k_{ro}} , \tag{3.2}$$

$$p_0 - p_w = p_{cap} , \tag{3.3}$$

where p_i, μ_i, v_i, and k_{ri} are the pressure, viscosity, Darcy velocity, and relative permeability of phase i, k is the absolute permeability, and p_{cap} is the capillary pressure; all these quantities are macroscopic variables, obtained by averaging the microscopic quantities over some suitable region. The position variable x denotes the distance from the inlet face of the sample. The physical idea behind the relative permeability concept embodied in these equations is that when two fluids are present in the medium the permeability to each phase is reduced because some of the flow channels are occupied by the other fluid. In order to implement this idea it is necessary to specify the functional dependence of the relative permeabilities k_{ri}, and also of the capillary pressure p_{cap}. The usual hypothesis is that these quantities depend only on how much of each fluid is present, i.e., they are unique functions of saturation. The correctness of this hypothesis can be substantiated theoretically, if at all, only by a detailed examination of length and time scales and/or a microscopic computer simulation which includes both viscous and capillary forces. Such an attempt is far beyond the scope of this paper; here we will merely point out two key assumptions implicit in the application of these ideas.

(1) At any given saturation, each fluid flows in its own set of flow channels and exerts negligible shear stress on the other fluid.

(2) From the microscopic point of view, the only effect of the bulk flow is to produce a local capillary pressure between the phases which evolves in time; the interface motions respond to this pressure difference in the same way as they would in the quasistatic limit. Under this assumption, the sequence of configurations that a given region passes through is independent of the bulk capillary number (only the rate at which these changes take place is altered) and it makes sense to assume that the relative permeabilities and capillary pressure are unique functions of saturation, independent of the flow rate. (While the above assumption is clearly sufficient to obtain this result, it seems to the present author that it is also necessary; if the actual fluid configurations at a given saturation depended on the flow rate which created them, it would seem most implausible that the relative permeabilities and capillary pressure would be functions only of saturation.) Thus the relative permeability and capillary pressure functions may be determined theoretically from a model which operates at infinitesimal flow rate, e.g., the $B=0$ version of the model considered in Sec. II. This basic idea has been advanced recently by Heiba, Sahimi, Scriven, and Davis,[18] although we would argue that invasion percolation is a better quasistatic model than ordinary percolation as assumed by these authors. We will not dwell on these differences here but merely note that the relative permeabilities and capillary pressure functions obtained in either case are in qualitative agreement with experiment, and of the typical form shown in Fig. 9.

Although we will provisionally adopt assumption (2), the main result of this section will be that in fact this assumption necessarily breaks down as the system approaches residual oil saturation. In order to see how this comes about we must examine the nature of the solutions to the Eqs. (3.1)–(3.3). In addition to these equations we have the mass balance equations for each phase

$$\frac{\partial}{\partial t}(\phi S_i) + \frac{\partial v_i}{\partial x} = 0 , \tag{3.4}$$

where ϕ is the porosity and the S_i are the fluid saturations. The initial condition is

$$S_w = 0 \quad \text{at } t = 0 \tag{3.5}$$

and the boundary condition at the inlet face is

$$v_0 = 0 \quad \text{at } x = 0 \tag{3.6a}$$

$$v_w = v \quad \text{at } x = 0 \tag{3.6b}$$

where v is the imposed Darcy velocity of the flow. In the absence of the capillary pressure term (3.3), we have the well-known Buckley-Leverett problem,[19] and the condition (3.6a) is satisfied by requiring $k_{ro}=0$ at $x=0$, i.e., $S_w = 1 - S^*_{or}$. In the presence of the capillary pressure term, however, the correct boundary condition is

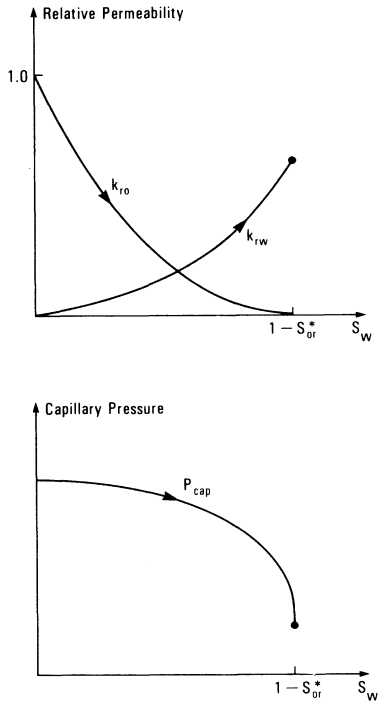

FIG. 9. Typical imbibition curves for water relative permeability k_{rw}, oil relative permeability k_{ro}, and capillary pressure p_{cap} as functions of the water saturation S_w. The arrows represent the direction of saturation change, i.e., increasing water saturation.

$$\frac{\partial p_0}{\partial x}=0\ , \tag{3.7}$$

a possibility which is excluded in the Buckley-Leverett problem because it would cause $\partial p_w/\partial x$ to vanish also. A typical solution to (3.1)—(3.7) is sketched in Fig. 10. At fixed position x, the water saturation S_w approaches $1-S^*_{or}$ as time $t\to\infty$. Just as in the buoyancy case we will find it useful to consider the allowed fraction q as a macroscopic variable. As the oil saturation at any position approaches residual, the value of q approaches $1-q_c$, i.e., Δq in (2.11) goes to zero. Eventually a situation is reached where the change in q over a correlation length is no longer small and, just as in the buoyancy case, it no longer makes sense to consider q as a macroscopic variable. It is clear that the inequality (2.12), or its equivalent

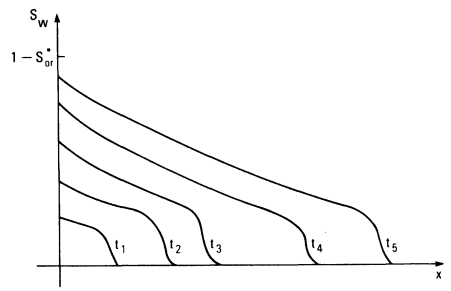

FIG. 10. Typical solutions of Eqs. (3.1)—(3.7) for the water saturation S_w as a function of position x, at various times $t_1<t_2<t_3<t_4<t_5$.

(2.14), is first violated at $x=0$, since the water saturation is always largest there. At $x=0$ we have from (3.3), (3.7), (3.1), and (3.6b)

$$\frac{\partial p_{cap}}{\partial x}=-\frac{\partial p_w}{\partial x}=\frac{\mu_w v}{k k_{rw}}\ . \tag{3.8}$$

Since we are considering small capillary numbers, i.e., small changes in the residual saturation, the relative permeability k_{rw} should be evaluated at $S_w=1-S^*_{or}$. Computing the maximum cluster size in the same way as in Sec. II, we obtain

$$\frac{L_{max}}{R}\sim\left[\frac{N_{cap}}{K_w}\right]^{\nu/(1+\nu)}, \tag{3.9}$$

where the suppressed factors of order unity are the same as in (2.17), N_{cap} is the capillary number (1.6), and the dimensionless constant K_w is given by

$$K_w=\frac{k k_{rw}}{R^2}\ . \tag{3.10}$$

If we assume that the effect of the cutoff in the blob size distribution on the residual saturation is the same as in the buoyancy case, we obtain

$$S^*_{or}-S_{or}\sim\left[\frac{N_{cap}}{K_w}\right]^{(1+\beta)/(1+\nu)}, \tag{3.11}$$

where again the suppressed factors are the same as in the buoyancy case (2.19). In the situation where both viscosity and buoyancy act, the contributions to $\partial p_{cap}/\partial x$ in (2.14) are additive, and the residual oil saturation should depend on the combination

$$N_{cap}+\frac{k k_{rw}}{R^2}B\ . \tag{3.12}$$

The conclusion that residual saturation should scale as some such linear combination of N_{cap} and B is in agreement with the experiments of Morrow and Songkran,[20] who find for their sphere pack materials the combination

$$N_{cap}+0.001\,41B\ . \tag{3.13}$$

Using the values given by Morrow and Songkran,

$$\frac{k}{R^2}=0.003\,17$$

and

$$k_{rw}=0.63\ , \tag{3.14}$$

yields a value 2.0×10^{-3} for K_w in (3.10), in reasonable agreement with the value 1.141×10^{-3} obtained by direct correlation of the experimental data for various capillary and Bond numbers.

IV. DISCUSSION

In this paper we have considered a simple model of quasistatic immiscible displacement in the presence of

buoyancy forces. The fundamental idea of the model is that the individual oil-water interfaces "see" only the local value of the capillary pressure, and for small Bond numbers are not affected by the pressure gradient. However, as residual oil saturation is approached, the clusters being produced become so large that they do begin to see the gradient in the pressure. The net effect is that the largest clusters are absent from the distribution and the residual oil saturation is reduced. The chief results obtained were the small B scaling behavior of the maximum cluster size and of the residual saturation, Eqs. (2.17) and (2.19). The reason for this focus was partly because, due to the distortion of individual interfaces, the model loses its validity if B is not small, but more importantly because such scaling laws are expected to be universal for any system which exhibits percolationlike behavior. For example, these results should not be affected by the inclusion of snap-off processes, provided these processes are triggered by some kind of instability controlled by the local value of the capillary pressure. Although we do not try to justify percolation ideas in detail, we would point out that the effects discussed here depend on the nature of the percolation threshold of the nonwetting, oil, phase. The actual model we consider exhibits percolation thresholds in both phases, but it is possible that this is an artifact of the model. It may be that in reality the wetting phase coats the grains of the material and hence is always continuous; on the other hand, it is generally accepted that at residual saturation the nonwetting phase is broken up into disjoint clusters so that in some sense the approach to residual saturation must be a percolation threshold.

The major advantage of percolation ideas in immiscible displacement is that they can provide qualitative understanding without great computational effort. However, it is important that claims made for the percolation approach are in accord with what actually happens in a simple model based on these concepts. For example, the idea that residual saturations are reduced at finite Bond number or capillary number because the largest clusters are missing is very appealing, but we have seen that the way in which this effect operates is much more complicated than one might imagine. This is partly due to the fact that the model, invasion percolation, is not exactly the same as ordinary percolation. Although we have argued that the scaling laws (2.17) and (2.19) can be understood in terms of ordinary percolation ideas, the arguments are somewhat complex, and one can take the more pragmatic view that on general grounds one would expect such universal scaling laws, and then obtain the critical exponents from computer simulations of the invasion percolation model in the presence of buoyancy. Such simulations are in any case not much more complicated than those of ordinary percolation. From this point of view, the fact that the critical exponents can be expressed in terms of percolation exponents is of merely academic interest.

The expected universality of the scaling laws means that they can provide crucial tests of the entire percolation approach, and hence to some extent of the assumed underlying pore level processes. While in artificial two-dimensional micromodels these processes can in principle be observed directly, in a real material this will probably never be possible, and one must rely on more macroscopic observations such as residual saturation and cluster size distribution. The former is a truly global measurement and does not require observations inside the system, but has the disadvantage that the scaling law (2.19) involves the deviation of the residual saturation from its $B=0$ value and so requires very accurate measurements; for this reason the data of Morrow and Songkran seems not of sufficient quality to estimate the exponent λ reliably. The maximum cluster size (2.17) requires internal measurements of the system, but is potentially more interesting because the predicted value 0.47 of the critical exponent μ is strikingly different from the naive value of unity. Unfortunately, all experiments involving buoyancy suffer from the disadvantage that the Bond number (1.11) is not easy to control. The experiments of Morrow and Songkran used a glass-sphere pack for the medium, and altered the sphere size R; this has the defect that changes in packing geometry can obscure the effects due to buoyancy. Alternatively one can alter the fluids to change the density difference $\Delta\rho$ or interfacial tension γ, but this runs the risk of changing the wettability characteristics. The ideal way to change the Bond number is to use a centrifuge to alter the effective acceleration g due to gravity; this is somewhat cumbersome but doubtless possible.

In Sec. III we suggested how the analysis might be extended to the case of pressure fields created by viscous rather than buoyancy effects. From the experimental point of view this is much simpler because the capillary number N_{cap} in (1.6) can be simply controlled by adjusting the flow rate. Even here, though, we know of no data which is of sufficient quality to test the predictions (3.9) and (3.11) accurately. In particular there exists no systematic data on the variation of cluster size distribution with capillary number. Qualitatively, however, the prediction that the maximum cluster size (3.9) should scale as something like the square root of the inverse capillary number is very important. For example, if the capillary number is 10^{-6} (a typical reservoir waterflood value), and the constant K_w is of order 10^{-3}, then (3.9) predicts a maximum cluster length of about 30 pore radii, as opposed to the naive estimate based on the capillary length (1.8) which is of the order of 1000 pore lengths. While typically clusters even as large as 30 pore radii are not reported, the prediction of this paper is certainly a great improvement over the naive estimate. Another interesting aspect of this prediction is that the clusters which are formed at a given capillary number are well below the mobilization length (at that capillary number), because the mobilization length is typically of the order of L_{cap}.[3,13] This can provide another explanation of the initial flatness of the disconnected oil curve a in Fig. 1 which would hold even if it were true that clusters were displaced from the sample once they were mobilized.

The theoretical situation in the viscous case is more complex because there is no simple model which takes into account the viscous effects. The analysis of this paper merely shows that if one accepts the mean-field picture in which each meniscus moves in the average pressure field due to the other motions, then effects similar to

the buoyancy case will occur as residual saturation is approached. One way to investigate the validity of these assumptions theoretically is to use computer simulations such as those of Koplik and Lasseter[21] or of Dias[22] which perform an exact calculation of the viscous pressure field at each step of the process, as well as keeping track of the interfacial pressure drops due to the individual oil-water menisci. Such a simulation naturally takes into account both the viscous pressure fields due to the local motions (which occur even in the absence of a bulk flow) and those due to the bulk flow itself, so that in practice it is not easy or even possible to separate these effects. Nevertheless, it is certainly possible in principle to examine whether the behavior of the maximum cluster size and of the residual saturation at low capillary numbers is in agreement with the scaling predictions (3.9) and (3.11). Unfortunately, due to computational complexity, these simulations are at present limited to somewhat small networks so that there is a limit to the range of capillary numbers which can be investigated. Furthermore, the networks are two-dimensional and therefore do not have the correct topological properties. Hopefully, improvements in the efficiency of the algorithms and in computational power will remedy these deficiences in the not too distant future.

ACKNOWLEDGMENTS

The author would like to thank P. Hammond, J. R. A. Pearson, and J. Willemsen for useful discussions, and B. Halperin for suggesting the line of argument used in the Appendix. Thanks are also due to P. Hammond, D. Johnson, L. Kadanoff, and T. Lasseter for critical readings of the manuscript.

APPENDIX

In this Appendix we investigate the effect of buoyancy on the residual oil saturation S_{or}. To do this we will first investigate the effect of a finite system size of linear size L, and then replace L by the maximum cluster length L_{max} obtained in (2.17). In this Appendix only, we will use the notation $p=1-q$ to denote the allowed oil fraction, where q is the allowed water fraction defined in Sec. II. Since we will be concerned with the connectedness properties of both phases, we will generically refer to the allowed fraction (occupation probability) as x, and denote the percolation threshold by x_c. The argument is based on properties of the percolation-theory order parameter $P(x)$, defined for an infinite system to be the fraction of occupied sites which are in the infinite cluster when the sites are randomly occupied with probability x. On a finite system of dimension L we may define an analogous quantity $P_L(x)$ if we identify the "infinite cluster" as those occupied sites connected to the boundary, or more appropriate for our case, those connected to the inlet (or outlet) face. Any such definition is expected to converge to $P(x)$ as $L\to\infty$. Typical curves are sketched in Fig. 11. We note that $P(x)$ and $P_L(x)$ differ appreciably only in the critical region close to x_c. Close to the critical point, $P(x)$ has the behavior

$$P(x)\sim(x-x_c)^{\beta}\,, \tag{A1}$$

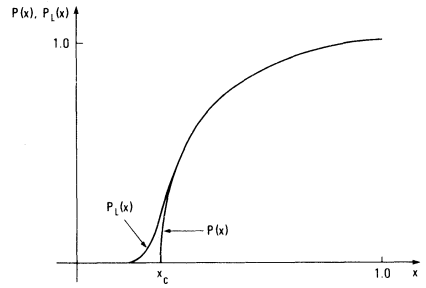

FIG. 11. Typical plots of the percolation-theory order parameter as a function of occupation probability x. The curve $P(x)$ represents an infinite system, and the curve $P_L(x)$ the analogous quantity on a system of finite size L. Note that the curves differ appreciably only in the critical region where the correlation length becomes large.

where $\beta\sim0.45$ is a universal critical exponent, while for $x\gg x_c$ we see that $P(x)$ quickly approaches unity, i.e., almost all the occupied sites are in the infinite cluster.

The point of view adopted here, as throughout this paper, is that invasion percolation in three dimensions can be understood in terms of ordinary percolation, provided one is careful to make the correct comparisons. In particular we must take careful account of the two main differences listed in Sec. II, namely, that the water in invasion percolation consists of only a single cluster, and that the water does not invade finite clusters of oil. In order to deal with the first point we observe that the important effects of a size cutoff L occur when the trapped oil clusters are becoming large, i.e., when the oil is approaching its percolation threshold and $q\sim1-x_c$. At this value of q it is reasonable to treat the water as a random q fraction as in ordinary percolation, since $P(q)$ is close to unity and the finite water clusters which would occur in ordinary percolation are very few and very small. Given this assumption the second point can be treated exactly. The key observation is that the way in which the infinite oil cluster is broken down does not depend on whether or not the water invades the finite oil clusters. Thus it is permissible to "imagine" that the water does, in fact, invade these clusters, provided one keeps track of how much of the water actually displaced oil from the infinite cluster. Let us consider the process of reducing the oil fraction from p to $p-dp$. The fraction of oil which is in the infinite cluster at this value of p is by definition $P(p)$ so that the water saturation increases by an amount

$$dS_w=P(p)dp\,. \tag{A2}$$

Thus at the end of the process the water saturation is

$$S_w=\int_0^1 P(p)dp\,, \tag{A3}$$

i.e., the residual oil saturation is

$$S_{or}^*=1-\int_0^1 P(p)dp\,. \tag{A4}$$

Since the same result holds for a finite system we obtain

$$S_{or}^*-S_{or}^*(L)=\int_0^1 [P_L(p)-P(p)]dp\,, \tag{A5}$$

where $S_{or}^*(L)$ is the residual saturation for a system of

linear size L. Actually, the result (A2) is only really correct when p is appreciably less than $1-x_c$, i.e., $q \gg x_c$, since only then is it reasonable to ignore the fact that the water is a single connected cluster as opposed to a random q fraction. However, we believe that this error will cancel in the difference (A5), so that (A5) does give the correct leading behavior in L. Since we see from Fig. 11 that the curves $P(p)$ and $P_L(p)$ differ only over an area near the critical point of width Δp and height Δp^{β}, where Δp scales as $L^{-1/\nu}$, we obtain

$$| S_{\rm or}^{*} - S_{\rm or}^{*}(L) | \sim L^{-(1+\beta)/\nu} , \tag{A6}$$

with $\beta \sim 0.45$ and $\nu \sim 0.88$.[16] Since the exponent in (A6) is large, of order 1.6, we see that the convergence of $S_{\rm or}^{*}$ to its asymptotic value for $L \to \infty$ is very rapid. Such rapid convergence is indeed seen in our simulations at $B=0$, though the quality of our data is not sufficient to obtain a good value for the exponent. Replacing the system size L by the cutoff $L_{\max}$ obtained in the buoyancy calculation we obtain the scaling form of the buoyancy dependence as

$$S_{\rm or}^{*} - S_{\rm or} \sim B^{(1+\beta)/(1+\nu)} , \tag{A7}$$

which is the result given in (2.19).

---

[1]Excluded from consideration here is the situation in which the displacing fluid has lower viscosity than the displaced fluid, where viscous fingering is an important effect.

[2]K. K. Mohanty, Ph.D. thesis, University of Minnesota, 1981; K. K. Mohanty, H. T. Davis and L. E. Scriven, Society of Petroleum Engineers Paper No. 9406, 1980 (unpublished).

[3]J. C. Melrose and C. F. Brandner, Can. J. Petrol. Tech. 13, 54 (1974).

[4]R. G. Larson, L. E. Scriven, and H. T. Davis, Chem. Eng. Sci. 36, 57 (1981).

[5]P. G. de Gennes and E. Guyon, J. Mech. 17, 403 (1978).

[6]R. Lenormand and S. Bories, C. R. Acad. Sci. 291, 279 (1980).

[7]R. Chandler, J. Koplik, K. Lerman, and J. Willemsen, J. Fluid Mech. 119, 249 (1982).

[8]J. Koplik, D. Wilkinson, and J. Willemsen, in *The Mathematics and Physics of Disordered Media* (Springer, Berlin-Heidelberg, 1983).

[9]D. Wilkinson and J. Willemsen, J. Phys. A 16, 3365 (1983).

[10]See, for example, I. Chatzis and N. R. Morrow, Society of Petroleum Engineers Paper No. 10114, 1981 (unpublished).

[11]Experimental evidence for this breakup has been observed by N. Wardlaw (private communication). For theoretical evidence in the form of computer simulations, see A. Payatakes, K. Ng, and R. Flumerfelt, AIChE J. 26, 430 (1980); A. Payatakes, Annu. Rev. Fluid Mech. 14, 365 (1982).

[12]Actually the knee in curve a of Fig. 1 occurs at somewhat lower capillary number than $K \sim 10^{-3}$. One explanation could be that the permeability in the definition (1.7) should not really be the absolute permeability, but rather the effective permeability to water when the oil has been broken up into small clusters; this will decrease the value of K. Another possibility is that the onset of oil production occurs when coalescence of oil ganglia (clusters) becomes important. See, for example, A. Payatakes, Ref. 11. In either case it remains true that the shape of curve a in Fig. 1 is not controlled simply by the size distribution obtained in percolation.

[13]R. G. Larson, H. T. Davis, and L. E. Scriven, Chem. Eng. Sci. 36, 75 (1981).

[14]W. B. Haines, J. Agric. Sci. 20, 97 (1930).

[15]B. Nickel and D. Wilkinson, Phys. Rev. Lett. 51, 71 (1983).

[16]D. W. Heermann and D. Stauffer, Z. Phys. B 44, 339 (1981); D. S. Gaunt and M. F. Sykes, J. Phys. A 16, 783 (1983).

[17]See for example, A. Scheidegger, *The Physics of Flow Through Porous Media* (University of Toronto, Toronto, 1974).

[18]A. A. Heiba, M. Sahimi, L. E. Scriven, and H. T. Davis, Society of Petroleum Engineers Paper No. 11015, 1982 (unpublished).

[19]S. E. Buckley and M. C. Leverett, Trans. AIME 146, 107 (1942).

[20]N. R. Morrow and B. Songkran, *Surface Phenomena in Enhanced Oil Recovery* (Plenum, New York, 1981), p. 387.

[21]J. Koplik and T. Lasseter, Society of Petroleum Engineers Paper No. 11014, 1982 (unpublished).

[22]M. M. Dias, Ph.D. thesis, University of Houston, 1984 (in preparation).